HHS Public Access

Author manuscript

Arch Biochem Biophys. Author manuscript; available in PMC 2017 August 15.

Published in final edited form as:

Arch Biochem Biophys. 2016 August 15; 604: 63–73. doi:10.1016/j.abb.2016.06.008.

(−)-RHAZINILAM AND THE DIPHENYLPYRIDAZINONE NSC 613241: TWO COMPOUNDS INDUCING THE FORMATION OF MORPHOLOGICALLY SIMILAR TUBULIN SPIRALS BUT BINDING APPARENTLY TO TWO DISTINCT SITES ON TUBULIN[1,,2]

Ruoli Bai and **Ernest Hamel**

Screening Technologies Branch, Developmental Therapeutics Program, Division of Cancer Treatment and Diagnosis, National Cancer Institute, Frederick National Laboratory for Cancer Research, National Institutes of Health, Frederick, Maryland 21702

Abstract

The most potent microtubule assembly inhibitor of newer diphenylpyridazinone derivatives examined was NSC 613241. Because NSC 613241 and (−)-rhazinilam also induce the formation of similar 2-filament spirals, these aberrant reactions were compared. Spiral formation with both compounds was enhanced by GTP and inhibited by GDP and by 15 other inhibitors of microtubule assembly. Similarly, microtubule assembly induced by paclitaxel or laulimalide is enhanced by GTP and inhibited by GDP and assembly inhibitors, but neither [^{3}H]NSC 613241 nor [^{3}H](−)-rhazinilam bound to microtubules or inhibited the binding of [^{3}H]paclitaxel or [^{3}H]peloruside A to microtubules. Differences in the pitch of aberrant polymers were found: NSC 613241-induced and (−)-rhazinilam-induced spirals had average repeats of 85 and 79–80 nm, respectively. We found no binding of [^{3}H]NSC 613241 or [^{3}H](−)-rhazinilam to αβ-tubulin dimer, but both compounds were incorporated into the polymers they induced in substoichiometric reactions, with as little as 0.1–0.2 mol compound/mol of tubulin, and no cross-inhibition by NSC 613241 or (−)-rhazinilam into spirals occurred. Under reaction conditions where neither compound induced spiral formation, both compounds together synergistically induced substantial spiral formation. We conclude that (−)-rhazinilam and NSC 613241 bind to different sites on tubulin that differ from binding sites for other antitubulin agents.

[1]This paper is dedicated to the memory of Dr. Larry J. Powers, in whose laboratory at Ricerca Corporation the diphenylpyridazinone derivatives were synthesized.

[2]The content of this paper is solely the responsibility of the authors and does not necessarily reflect the official views of the National Institutes of Health. The authors have no conflicts of interest to disclose.

Address correspondence to Dr. Ernest Hamel, Building 322, Room 102, Frederick National Laboratory for Cancer Research, Frederick MD 21702. Telephone: 301-846-1678, FAX: 301-846-6014, hamele@mail.nih.gov.

Keywords

Diphenylpyridazinone derivatives; NSC 613241; (−)-Rhazinilam; Tubulin polymer of aberrant morphology; Inhibition of tubulin assembly; Glutaraldehyde-fixed microtubules

1. Introduction

Microtubules and tubulin continue to be an important target for cancer therapy. Newer clinically approved agents that interfere with the function of these organelles are the epothilone analogue ixapebilone [1], the halichondrin B analogue eribulin [2], and the taxoid cabazitaxel [3]. The tubulin-microtubule equilibrium has become a major target for antibody-drug conjugates, with brentuximab vedotin (a complex containing a dolastatin 10 analogue) and ado-trastuzumab emtansine (a complex containing a maytansinoid) being recently approved for use in patients expressing the appropriate antigens on their tumors [4,5]. These antibody-drug conjugates contain analogues of highly cytotoxic natural products that failed to demonstrate sufficient antitumor activity at acceptable doses in human patients.

Tubulin and microtubules contain a variety of binding sites for agents that interfere with either their assembly or disassembly. However, a number of compounds interact at sites that are ill-defined, in comparison with more well-defined binding sites, such as those for colchicine [6] and paclitaxel [7]. Two examples of such compounds (structures in Fig. 1) are (−)-rhazinilam [8], derived from a natural product, and the synthetic diphenylpyridazinones (DPPs[3]) [9]. These agents appear to be related to each other in that they each cause aberrant assembly reactions with formation of well-defined spiral structures of similar morphology [8–10]. In addition, both (−)-rhazinilam and the DPPs can inhibit tubulin assembly in vitro at substoichiometric concentrations, relative to the amount of tubulin in the reaction mixture [9,10]. Inhibition occurs with lower compound concentrations than those required for spiral formation.

(−)-Rhazinilam was isolated from plants of the *Apocynaceae* family. Not a true natural product, it is formed by rapid degradation of the original natural product [11,12]. Cells treated with (−)-rhazinilam show IC_{50} values for the compound in the low μM range [8,10,12,13], as compared with nM and pM IC_{50}'s for the most potent antitubulin agents. Cells treated with (−)-rhazinilam show the typical mitotic arrest observed with antitubulin compounds. Most strikingly, despite the inhibition of assembly and the aberrant assembly reaction described above, cells treated with (−)-rhazinilam show the bundled microtubules observed with paclitaxel and other taxoid site agents [8]. During an analysis of effects obtained with (−)-rhazinilam analogues, we observed that if GTP was omitted from the reaction mixture, both microtubules and the characteristic spirals were formed, in approximately equal amounts [10]. We then performed extensive experiments, so far without success, to find reaction conditions that would tip the assembly balance further in the direction of microtubules.

[3]*Abbreviations used:* DPP, diphenylpyridazinone; HPLC, high-performance liquid chromatography; MAPs, microtubule-associated proteins; Mes, 4-morpholineethanesulfonate; gMTs, glutaraldehyde-fixed microtubules.

The original DPP compounds were synthesized as antihypertensives [14,15], and some of them had herbicidal activity [16]. In a toxicological study, mitotic figures were found in renal tissue [17,18]. In our laboratory, we examined many DPPs for interactions with tubulin [9]. The most active compounds caused mitotic arrest in cultured cells, although, like (−)-rhazinilam, IC_{50}'s were generally about 1 μM. Since our original study, additional DPPs were synthesized, and some had greater antitubulin activity than the original compounds, but maximum cytotoxicity was unchanged (unpublished observations).

Intrigued by the similarities between (−)-rhazinilam and the DPPs in their effects on tubulin, we arranged for the synthesis of [^{3}H](−)-rhazinilam and [^{3}H]NSC 613241, which was the DPP derivative with the greatest inhibitory effect on tubulin assembly. We also performed comparative studies on the aberrant assembly reactions. Our goal was to gain insight into the binding sites for these compounds on tubulin.

2. Materials and methods

2.1. Materials

The DPP derivatives were synthesized in the laboratory of the late Dr. Larry J. Powers of Ricerca Biosciences, Concord, Ohio. High-performance liquid chromatography (HPLC) analyses indicated > 99% purity of NSC 613241 and 92% purity of NSC 608593. (−)-Rhazinilam was a generous gift of Dr. F. Guéritte, Centre National de la Recherche Scientifique, Gif-sur-Yvette, France. HPLC analysis indicated 96% purity. The racemic rhazinilam analogue shown in Fig. 1 was generously provided by Dr. W. G. Bornmann, University of Texas M. D. Anderson Cancer Center. Podophyllotoxin and nocodazole were from Aldrich. All DPPs were provided by the Developmental Therapeutics Program, National Cancer Institute compound repository, as were paclitaxel, [^{3}H]paclitaxel (16. 2 Ci/mmol; radiochemical purity 97% on two TLC and one HPLC analysis), vinorelbine, vinblastine, vincristine, and maytansine. Synthetic laulimalide and peloruside A were generous gifts of Dr. A. Ghosh, Purdue University. Combretastatin A-4, dolastatins 10 and 15, halichondrin B, and spongistatin 1 were generous gifts of Dr. G. R. Pettit, Arizona State University. Thiocolchicine was a generous gift of the late Dr. Arnold Brossi, National Institute of Diabetes and Digestive and Kidney Diseases. Epothilone B and cryptophycin 1 were generously provided by Merck Research Laboratories. The pentapeptide *N*,*N*-dimethylvalyl-valyl-*N*-methylvalyl-prolyl-proline was a generous gift of the Genzyme Corporation. This pentapeptide has been found to be formed intracellularly from dolastatin 15, as well as from related synthetic analogues (such as cemadotin and tasidotin), as a metabolite more active than the parental depsipeptides [19,20] as an antitubulin agent. The isolation of hemiasterlin was described previously [21]. [^{3}H](−)-Rhazinilam (7.0 Ci/mmol; radiochemical purity 97.5% on two TLC and one HPLC analysis), [^{3}H]NSC 613241 (1.4 Ci/mmol; radiochemical purity 98% on two TLC and one HPLC analysis), and [^{3}H]peloruside A (1.2 Ci/mmol; radiochemical purity 97% on two TLC and one HPLC analysis) were prepared from the nonradiolabeled compounds by AmBios Laboratories. Electrophoretically homogenous bovine brain tubulin and microtubule-associated proteins (MAPs) were prepared as described previously [22], including removal of unbound nucleotide from the tubulin by gel filtration chromatography [23].

2.2. Methods

Turbidity development in tubulin solutions at 350 nm was followed in Gilford model 250 recording spectrophotometers equipped with electronic temperature controllers. Temperature increases at about 0.5 °C/s. All reaction components except tubulin and compounds of interest were thoroughly mixed in cuvettes that were held a 0 °C in the spectrophotometer. Tubulin was mixed into the reaction mixtures, and baselines were established. Compounds, dissolved in dimethyl sulfoxide, were next mixed into the reaction mixtures, and, if necessary, baselines were reestablished. The reaction was followed sequentially for 20 min each at 0, 10, and 20 °C, unless otherwise indicated. Sometimes, aliquots were removed from the reaction mixtures for electron microscopy. The 0.25 mL reaction mixtures contained 0.6 M monosodium glutamate (from a 2.0 M stock solution adjusted to pH 6.6 with HCl), 1.0 mg/mL (10 μM) tubulin, 1.0 mM $MgCl_2$, 50 μM GTP, 2% (v/v) dimethyl sulfoxide, unless indicated otherwise, and compounds as indicated.

For electron microscopy, about 10 μL of a reaction mixture was placed on a 200-mesh carbon-coated, Formvar-treated copper grid and immediately stained with several successive drops of 1% (w/v) uranyl acetate, with excess stain wicked from the grid with torn filter paper. The grids were examined in a Zeiss model 10CA electron microscope.

In some experiments, compound effects were studied in an assembly system in which MAPs were required for tubulin polymerization. Reaction mixtures contained 1.0 mg/mL tubulin, 0.5 mg/mL MAPs purified by DEAE-cellulose chromatography, 1.0 mM GTP, 0.1 M Mes (taken from a 1.0 M stock solution adjusted to pH 6.9 with NaOH), 0.5 mM $MgCl_2$, and 2% dimethyl sulfoxide as compound solvent. Assembly was at 37 °C for 20 min, with extent of the reaction the parameter measured for determination of IC_{50} values.

Binding of drugs to microtubules was measured with glutaraldehyde-fixed microtubules (gMTs), prepared as described by Díaz et al. [24]. Reaction details are described in Table 2.

Binding of [^{3}H](−)-rhazinilam and [^{3}H]NSC 613241 to tubulin was examined by several techniques. These included centrifugal gel filtration [25] and size exclusion HPLC [26], neither of which was useful. We therefore evaluated incorporation of the radiolabeled compounds into the spiral polymers, which were harvested by ultracentrifugation. Reaction mixtures (100 μL volume) contained 0.6 M monosodium glutamate (pH 6.6), 1.0 mg/mL tubulin, 1.0 mM $MgCl_2$, 50 μM GTP, 2% dimethyl sulfoxide, and compounds as indicated. Samples were incubated at room temperature (about 22 °C) for 30 min, then centrifuged at 45,000 rpm for 10 min at 22 °C. A TLA 55 rotor and an Optima TLX ultracentrifuge from Beckman Instruments were used. The supernatants were discarded, and the pellets were dissolved in 0.25 mL 8.0 M urea. Protein (Lowry reaction) and radiolabel were determined on 100 μL of the urea solutions. For stoichiometry determinations (compound/tubulin) a molecular weight of 100 kDa was used for tubulin, based on the primary sequences of α- and β-tubulin [27,28].

In ultacentrifugation experiments with nonradiolabeled drugs, GTP was not included in the reaction mixtures, incubation was for 20 min at 0 °C, and centrifugation was at 2 °C. The dimethyl sulfoxide concentration was 4%. Protein concentration was determined on the

supernatants, and the amount of polymer formed was determined by subtraction from the protein concentration of uncentrifuged reaction mixtures.

3. Results

3.1 Inhibition of MAP-dependent microtubule assembly by newer DPPs and by (−)-rhazinilam

Previously [9], IC_{50}'s for microtubule assembly for the most active DPPs were determined to be 5–10 μM. When determined more precisely, the compound that yielded the lowest IC_{50} was NSC 362455 (5.8 ± 0.23 [SD] μM). In terms of structure-activity relationships, the substituent at N-2 had unpredictable effects on activity, the nitrile group at C-4 was important, an analogue lacking both phenyl rings was inactive, and chlorine substituents on the phenyl rings enhanced activity. Among newer analogues, three had greater activity than NSC 362455: NSC 613241 (IC_{50}, 2.5 ± 0.13 μM), NSC 608593 (IC_{50}, 3.0 ± 0.23 μM), and NSC 614930 (IC_{50}, 4.2 ± 0.076 μM). Thus, fluorine substituents, like chlorine substituents, on the phenyl rings modestly enhanced activity (see Fig. 1). The methyltetrazole substituent at N-2 was the best alkyl group of those examined. Two analogues of NSC 362449, each missing one of the two phenyl rings, had no significant effect on microtubule assembly (NSC 608602 lacked the phenyl ring at C-5, NSC 608600 at C-6).

With different tubulin and MAPs preparations, we examined the effects of (−)-rhazinilam on microtubule assembly, in comparison with NSC 613241, obtaining IC_{50} values of 1.9 ± 0.11 and 2.3 ± 0.071 μM for NSC 613241 and (−)-rhazinilam, respectively. The turbidity tracings indicated that aberrant assembly reactions (reactions that were not cold reversible) occurred with as little as 2.0 μM NSC 613241 and 3 μM (−)-rhazinilam at 37 °C. With either compound at 20 μM, there was aberrant assembly at 0 °C, with a slight further increase in turbidity at 37 °C.

3.2. Induction of spiral formation in reaction mixtures containing glutamate but not MAPs

We had found that (−)-rhazinilam induced partial microtubule formation in reaction mixtures containing 0.75 M monosodium glutamate but no GTP [10]. Adding GTP significantly enhanced the aberrant assembly reaction, but only spirals were formed. Many experiments aimed at generating (−)-rhazinilam-induced microtubules and no spirals were unsuccessful, including adding GDP to the reaction mixture. We should also note that use of glutamate to induce tubulin assembly eliminates the confounding problem of MAPs in the reaction mixture, because inclusion of MAPs raises the possibility of a drug reaction with MAPs or with a MAPs-tubulin complex.

For comparative studies, we selected NSC 613241, the most active of the DPP derivatives. Under all glutamate-based conditions we examined, as well as in MAP-dependent assembly, NSC 613241 was more active than (−)-rhazinilam in inducing aberrant assembly reactions, even at 0 °C. We found that aberrant assembly at 0 °C was delayed for about 1 min following addition of NSC 613241 with 0.6 M monosodium glutamate, supplemented with 50 μM GTP, 1 mM $MgCl_2$, and 2% dimethyl sulfoxide.

In the experiments summarized in Fig. 2, all reaction mixtures contained tubulin and either NSC 613241 (Panel A, curves 1–4) or (−)-rhazinilam (Panel B, curves 5–8) at 10 μM, together with 0.6 M glutamate and 2% dimethyl sulfoxide. With both compounds, GTP dramatically enhanced the assembly reactions, and the reactions were further enhanced by $MgCl_2$, especially with (−)-rhazinilam (compare curves 7, without Mg^{2+}, and 8, with Mg^{2+}). Addition of 500 μM GDP to the complete reaction mixtures was inhibitory with both compounds (dashed curves 4a and 8a). In the absence of GTP, $MgCl_2$ had no effect on the reaction induced by NSC 613241 (compare curves 1 and 2) and inhibited the weak reaction induced by (−)-rhazinilam (compare curves 5 and 6). In 0.6 M glutamate, while not essential, GTP strongly enhanced the aberrant assembly reactions with both (−)-rhazinilam and NSC 613241.

The experiments presented in Fig. 2 were performed in temperature steps, about 20 min each at 0, 10, 20, and 30 °C. Generally, there was little change following the 30 °C step, so this phase of the reaction is not shown (but see Supplemental Figures 2–4). The reaction represented by curve 4 began shortly after adding the NSC 613241 to the reaction mixture held at 0 °C. Within 20 min at 0 °C the reaction was at about 30–35% of its maximum, with the reaction reaching about 90% of maximum at 10 °C. The comparable study with (−)-rhazinilam (curve 8) showed little or no change in turbidity after 20 min at 0 °C, reaching 75–80% of maximum at 10 °C, with a further increase at 20 °C, reaching the same turbidity level as occurred with NSC 613241. Without compound there was no change in turbidity (curves 4b and 8b).

The temperature difference observed with the two compounds did not derive from a difference in affinity for tubulin. Increasing compound concentrations to 20 μM had little effect on turbidity development under this reaction condition. With 20 μM (−)-rhazinilam, the reaction rate was somewhat faster than with 10 μM compound at 10 °C, but there was still almost no reaction at 0 °C.

The GTP requirement observed in these experiments could be reduced by changing the concentrations of the reaction components. Even more dramatic, it practically disappeared if (−)-rhazinilam and NSC 613241 were both added to the reaction mixtures (see below).

3.3. Aberrant polymer morphologies

Figs. 3 and 4 present electron micrographs of negatively stained polymer formed with (−)-rhazinilam or with NSC 613241, respectively, under the reaction conditions used in the studies presented in Fig. 2, following the 0 to 10 to 20 °C transitions. The morphologies observed here did not differ significantly from those described previously [9,10].

With (−)-rhazinilam, there were many areas on the grids where multiple, relatively short spiral structures were observed (Fig. 3A). There were also many densely stained structures from which single spirals seemed to peel off at the periphery (Fig. 3B). The pitch of the spirals seemed relatively irregular, but, in the highest magnification views obtained (Fig. 3C), a two filament substructure (arrow) was clearly observed. We also pretreated the (−)-rhazinilam structures with glutaraldehyde (0.2%) before applying them to a grid, and this maneuver made the spirals more regular in appearance (Fig. 3D). The glutaraldehyde-fixed

spirals had a mean pitch of about 79 nm. Non-fixed spirals yielded a similar pitch (mean, 80 nm).

With NSC 613241, there were also many areas where multiple spiral structures were crowded together (Fig. 4A). They were denser than was the case with (−)-rhazinilam and, perhaps somewhat longer. As with (−)-rhazinilam, there were also dense structures with single spirals peeling off at the periphery (Figs. 4B and 4C). Generally, the images, particularly at higher magnification (Fig. 4D), were less sharp than those obtained with (−)-rhazinilam, and no improvement was observed with a glutaraldehyde treatment. Nonetheless, a filamentous substructure was observed. Two filament structures are indicated by the single arrows. In other structures (double arrow), there is a suggestion of a three filament substructure, but this may be caused by overlapping spirals. The mean pitch of the spirals was 85 nm, somewhat larger than the pitch obtained with the (−)-rhazinilam structures.

In summary, the (−)-rhazinilam-induced structures stain with uranyl acetate more readily than those formed with NSC 613241 (i.e., sharper images were obtained) and had a somewhat shorter pitch. The (−)-rhazinilam structures, but not the NSC 613241 structures, took on a more regular appearance following glutaraldehyde treatment.

We should stress that the spirals formed with both (−)-rhazinilam and NSC 613241 differ markedly from those formed in the presence of vinblastine (Fig. 5), whether in the absence (Panel A) or presence of GTP (Panel B). We have generally found that in glutamate the vinblastine-induced spirals are tightly coiled, making determinations of pitch impossible, at least by methods available to us. However, in our micrograph collection we did find one vinca-induced structure (Supplemental Materials Fig. 1) with loops of individual coils that could be measured. We obtained an average pitch from this structure of 27 nm, but we are unable to appreciate a filament substructure in these spirals.

We should also note that many workers have studied vinca alkaloid-induced spirals over the years, and variations in structures and in the tightness of the coils have been described. MAPs in sulfonate buffers clearly affect polymer morphology (see ref. 26 for an example from our studies), but, as far as we know, no morphological differences have been observed with guanine nucleotides. Workers have described stronger aberrant assembly reactions with GDP vs GTP (e.g., ref. 29,30), but others have noted a requirement for GTP in the aberrant assembly reaction [31]. Variations in the tightness of the spirals formed are clear from published electron micrographs, but in only one report [32] was pitch measured. These workers found a repeat of 26–30 nm, depending on reaction conditions. This agrees with what we found in the micrograph presented in Supplemental Materials Fig. 1, but these workers noted a two filament substructure [32]. In contrast, Jordan et al. [33] observed vinblastine-induced disassembly of microtubules, and the spirals they observed were similar in appearance to those shown in Fig. 5 and in Supplemental Materials Fig. 1. Because multiple spirals were observed contiguous with microtubule ends, Jordan et al. [33] interpreted each spiral as being derived from a microtubule protofilament, and no filament substructure was described.

3.4. Effects of other compounds that inhibit microtubule assembly on spiral formation with 10 μM (−)-rhazinilam or 10 μM NSC 613241

We examined the effects of 15 inhibitors of microtubule assembly at 50 μM on the aberrant assembly reactions induced by either (−)-rhazinilam or NSC 613241 at 10 μM. In all cases, whether or not the inhibitor itself induced an aberrant assembly reaction (examples: vinblastine and dolastatin 10), the (−)-rhazinilam and NSC 613241 reactions were inhibited. This was especially obvious at the lower reaction temperatures. Our results are summarized in Table 1, and the turbidity tracings on which these conclusions are based are shown in the Supplemental Materials Figures 2–5. These inhibitory effects are reminiscent of the inhibition by many of these compounds on assembly induced by the microtubule stabilizing agents paclitaxel, epothilone B, discodermolide, and laulimalide [34,35]. In addition, spiral formation by (−)-rhazinilam and NSC 613241, like microtubule assembly with taxoid and laulimalide site agents [35,36; unpublished data], is enhanced by GTP and inhibited by GDP.

3.5. (−)-Rhazinilam and NSC 613241 did not inhibit the binding of [^{3}H]paclitaxel or [^{3}H]peloruside A to gMTs, and [^{3}H](−)-rhazinilam and [^{3}H]NSC 613241 did not bind avidly to gMTs

In addition to their inhibitory effects on the assembly of purified tubulin with and without MAPs and their induction of aberrant assembly reactions, both (−)-rhazinilam and DPP derivatives are unusual antimitotic agents in that they can induce formation of tubular structures. We found that (−)-rhazinilam could induce partial formation of microtubules [10] from purified tubulin, while David et al. [8] observed bundled microtubules in (−)-rhazinilam-treated cells. The finding that DPP derivatives have herbicidal activity led to studies in plants that included the observation in root tip tissue that the disappearance of microtubules was accompanied by the appearance of macrotubules that were 75 nm in diameter [9]. These polymerization effects raised the possibility that (−)-rhazinilam or NSC 613241 might bind in one of the two sites on microtubules occupied by microtubule stabilizing agents [37].

Morphological observations combining either compound with either a taxoid site or a laulimalide site compound were inconclusive. Adding either epothilone B or laulimalide to the spirals induced by (−)-rhazinilam or NSC 613241 led to formation of a variety of disorganized structures (see Supplemental Materials Figs. 7–9), with an occasional structure that seemed to have a protofilament substructure (Supplemental Materials Fig. 9). Adding either (−)-rhazinilam or NSC 613241 to microtubules induced by laulimalide or epothilone B led to persistence of the preformed microtubules (see Supplemental Materials Figs. 6–8).

We thought that the gMTs that have been extremely useful in evaluating taxoid site compounds [24] might provide information about potential binding sites for (−)-rhazinilam and/or NSC 613241. These experiments were negative. As shown in Table 2, neither compound in 10-fold molar excess inhibited the binding of either [^{3}H]paclitaxel or [^{3}H]peloruside A to gMTs. The control compounds, epothilone B and laulimalide, inhibited [^{3}H]paclitaxel and [^{3}H]peloruside A binding, respectively.

Neither [^{3}H](−)-rhazinilam nor [^{3}H]NSC 613241 had significant affinity for the gMTs, Binding stoichiometries were less than 0.04/tubulin in the gMTs, in contrast to the stoichiometries of 0.53 obtained with [^{3}H]paclitaxel and of 0.67 obtained with [^{3}H]peloruside A (Table 2).

3.6. Binding of [^{3}H](−)-rhazinilam and [^{3}H]NSC 613241 to aberrant tubulin polymer

We were unable to demonstrate binding of either [^{3}H](−)-rhazinilam or [^{3}H]NSC 613241 to the αβ-tubulin dimer. We therefore explored their incorporation into spiral polymers harvested by centrifugation. Relatively low concentrations of either agent led to large polymer pellets (Fig. 6A). With 10 μM tubulin, 5 μM compound led to pellets containing 73% of the tubulin with NSC 613241 and 53% with (−)-rhazinilam. In keeping with the apparently greater activity of NSC 613241 in inducing spiral formation, the DPP compound was more active than (−)-rhazinilam, in that a larger pellet was formed with the former as compared with the latter compound. At 20 μM, with both compounds the pellets contained about 90% of the tubulin in the reaction mixtures.

When incorporation of radiolabeled compounds into the pellets was examined, there was little apparent difference between them, and the stoichiometry of compound incorporation versus the amount of tubulin in the pellet was low (Fig. 6B). When compound and tubulin were equimolar (10 μM each), the stoichiometry of compound to tubulin in the pellets was 0.13 for [^{3}H](−)-rhazinilam and 0.11 for [^{3}H]NSC 613241. The stoichiometry of compound incorporation into the aberrant polymers rose as compound concentration increased, reaching maxima of 0.68 for (−)-rhazinilam and 0.62 for NSC 613241 at 80 μM. A slightly higher stoichiometry occurred with (−)-rhazinilam than with NSC 613241.

Both compounds induced substantial aberrant assembly reactions at substoichiometric concentrations. Combining the data of Figs. 6A and 6B, with 5 μM (−)-rhazinilam, stoichiometry in the polymer pellet was 0.13, with the pellet containing 53% of the tubulin in the original reaction mixture. This was even more dramatic with 5 μM NSC 613241, with stoichiometry 0.11 and 73% of the tubulin in the pellet. With 40 μM compound, nearly 100% of the tubulin was in the polymer with both compounds, and less than half the tubulin in the pellets had bound compound – stoichiometries were 0.47 and 0.42 tubulin with (−)-rhazinilam and NSC 613241, respectively.

With the radiolabeled ligands, we were unable to demonstrate cross inhibition of incorporation of either NSC 613241 or (−)-rhazinilam into spirals. An example of such an experiment is shown in Table 3. There was no definite inhibition by one ligand of the incorporation of the other into polymer. Addition of the nonradiolabeled ligand in both cases caused a significant increase in polymer formed.

3.6. Apparent synergy of (−)-rhazinilam and NSC 613241 in inducing spiral formation under “restrictive” reaction conditions

We previously demonstrated synergy between all taxoid site compounds and both laulimalide site compounds in any combination in inducing microtubule assembly, but this required finding restrictive reaction conditions where single compounds had little or no activity [38]. This observation bolstered the argument for separate binding sites on

microtubules predicted by the failure of laulimalide to inhibit the binding of taxoids to microtubules [39], subsequently confirmed by X-ray crystallography [37]. Could an analogous observation be made with NSC 613241 and (−)-rhazinilam?

Such experiments at 0 °C were undertaken in the absence of GTP. Fig. 7A shows a centrifugation study with 10 μM tubulin and (−)-rhazinilam alone, NSC 613241 alone, or a mixture of both compounds at concentrations up to 30 μM. Spiral formation was minimal with either compound alone but extensive with both compounds at 10 μM and above. Fig. 7B shows a turbidity experiment with the compounds at 15 μM, either separately or together, and of the individual compounds at 30 μM.

We explored this potential synergy further by examining combinations of the DPP derivatives NSC 613241 and NSC 608593 and of (−)-rhazinilam and an active rhazinilam analogue (structure in Fig. 1). The analogue was a racemic mixture, only one of which is probably active [10], so it was used at twice the concentration of the other compounds. The data in Table 4 show that spiral formation at 0 °C required the presence of both a DPP derivative and (−)-rhazinilam or the rhazinilam analogue.

4. Discussion

The predominant effect of interactions of (−)-rhazinilam and the DPP derivative NSC 613241 with tubulin appeared to be similar, induction of spiral polymers of apparently identical morphology. This suggested the compounds likely interacted at the same site on tubulin despite their disparate chemical structures. To demonstrate this unambiguously, we obtained radiolabeled versions of both compounds, and we studied the aberrant assembly reactions in greater detail.

We selected a reaction condition that reduced the rapid assembly induced by NSC 613241 at 0 °C. The assembly reactions were markedly enhanced by GTP and inhibited by GDP. Both aberrant assembly reactions were inhibited by all classes of agents that inhibit microtubule assembly. Taken together, these findings were highly reminiscent of the effects of taxoid site agents and of laulimalide on tubulin assembly into microtubules (assembly reactions enhanced by but not absolutely dependent on GTP, inhibited by GDP, and inhibited by drugs that inhibit microtubule assembly). The idea that (−)-rhazinilam, especially, might bind to a site on microtubules was appealing because of our finding [10] that, under at least one reaction condition, partial formation of microtubules from purified tubulin was induced by (−)-rhazinilam, and the agent can induce microtubule bundles in cultured cells [8]. Using gMTs, however, we found no evidence that either [^{3}H](−)-rhazinilam or [^{3}H]NSC 613241 bound readily to microtubules, while the gMTs avidly bound [^{3}H]paclitaxel and [^{3}H]peloruside A to the taxoid and laulimalide sites, respectively.

There was a difference in the pitch of the spirals formed with (−)-rhazinilam and NSC 613241, and they differed in how readily they stained with uranyl acetate. Those formed with (−)-rhazinilam were better visualized with uranyl acetate and had a pitch of 79–80 nm. The NSC 613241 structures were less clearly stained, and their pitch was 85 nm.

We were not able to demonstrate significant binding of either radiolabeled compound to the αβ-tubulin dimer, but both radiolabeled compounds were incorporated into polymer harvested by ultracentrifugation. With both compounds, we found that the aberrant assembly reactions were substoichiometric in that polymer contained relatively low amounts of compound as compared with its tubulin content. Moreover, we found that we were not able to prevent incorporation of [^{3}H](−)-rhazinilam into polymer with nonradiolabeled NSC 613241 nor of [^{3}H]NSC 613241 with nonradiolabeled (−)-rhazinilam. Although this could be a result of our not being able to achieve saturating concentrations of nonradiolabeled compound in view of the substoichiometric aberrant assembly reactions, it nevertheless seems most likely that (−)-rhazinilam and NSC 613241 bind to different sites on tubulin with a similar morphological outcome, reminiscent of what happens with taxoid and laulimalide site agents.

We further explored the two site possibility by examining a restrictive reaction condition where neither (−)-rhazinilam, an active rhazinilam analogue, nor the DPP derivatives NSC 613241 and NSC 608593 induced aberrant polymer formation alone. The two DPP derivatives together and (−)-rhazinilam combined with the rhazinilam analogue were also inactive. In contrast, significant polymer formation occurred when the two classes of drugs were used together in any combination. This synergy was parallel to what was observed previously when laulimalide or peloruside A was combined with a wide variety of taxoid site agents under restrictive reaction conditions where a single agent had little activity, even when combined with another agent of the same class [38].

We cannot exclude the possibility that (−)-rhazinilam and/or NSC 613241 might bind to one of the sites that accommodate inhibitors of microtubule assembly. We considered exploring this with our radiolabeled compounds. However, the studies presented above, showing that all inhibitors, no matter the binding site, inhibit both aberrant assembly reactions make this difficult, if not impossible, to study. One might also argue that the differences in inhibitor effects on the two aberrant assembly reactions (Table 1) further supports the conclusion that (−)-rhazinilam and DPP derivatives must bind to two different sites on tubulin.

We have no specific information that indicates where on the αβ-tubulin dimer either (−)-rhazinilam or NSC 613241 might bind. The (−)-rhazinilam- and DPP-induced spirals are very different morphologically from those induced by the vinca alkaloids, as shown above. Nevertheless, the crystal structures of tubulin with bound vinblastine [40] or a bound dolastatin 10 analogue [41,42] strongly suggest that the binding sites of compounds that induce aberrant assembly reactions are generated by the interaction of two tubulin dimers. In these crystals, the binding sites are formed by the interaction of α-tubulin on one dimer with β-tubulin on a second dimer. This was predicted in the pioneering work of Timasheff [43], who argued on kinetic grounds that the apparent biphasic Scatchard plots for radiolabeled vinca alkaloid binding to tubulin did not indicate two binding sites but cooperativity of tubulin αβ-dimers in binding the vinca alkaloids. We observed [26] the same phenomenon in the binding of [^{3}H]dolastatin 10 to tubulin, together with observing that the radiolabeled dolastatin 10 was bound initially to a 200 kDa species, presumably two αβ-dimers.

However, compounds binding in the αβ interface between two dimers generally inhibit tubulin-dependent GTP hydrolysis, while DPPs [9] enhance GTP hydrolysis, as do many, but not all, compounds binding in the colchicine site located at the αβ interface within a tubulin dimer [6]. It is unlikely that (−)-rhazinilam would inhibit GTP hydrolysis, since the effect of the compound on spiral formation, like that of NSC 613241, was strongly inhibited by GDP. These effects on GTP hydrolysis could indicate that (−)-rhazinilam and DPP derivatives bind to a site on β-tubulin, as do paclitaxel and laulimalide [7,37], both of which induce assembly reactions with nucleotide properties similar to those observed with (−)-rhazinilam and NSC 613241.

In closing, we should note that some of the observations reported here with (−)-rhazinilam were reported previously by David et al. [8]. They found that vinblastine and maytansine, but not colchicine, inhibited the aberrant assembly reaction, while we found that the tubulin-thiocolchicine complex had a reduced ability to form aberrant polymer. We also found complete inhibition of spiral formation by podophyllotoxin and partial inhibition by combretastatin A-4 and nocodazole, three well-characterized colchicine site agents. David et al. [8] also described a GTP requirement for spiral formation, although they did not point out that GTP was not a mandatory requirement for the reaction, probably because of differences in reaction conditions. With [^{3}H](−)-rhazinilam, they found binding to tubulin spirals but not to αβ-dimer, as did we, and even at high compound concentrations binding to tubulin was substoichiometric for them, too. David et al. [8] also mentioned experiments they had performed with unspecified DPP derivatives. In contrast to the dramatic spiral formation we observed with NSC 613241 at 0 °C, and spiral persistence at higher temperatures (also cf. ref. 9), David et al. [8] reported that spiral formation did not occur at 37 °C. They also described differing effects of DPP derivatives and (−)-rhazinilam on preformed microtubules, but we have not performed any analogous studies here with preformed microtubules.

Supplementary Material

Refer to Web version on PubMed Central for supplementary material.

References

1. Toppmeyer DL, Goodin S. Am J Clin Oncol. 2010; 7:516–521. [PubMed: 20023567]
2. Gradishar WJ. Curr Oncol Rep. 2011; 13:11–16. [PubMed: 21104168]
3. Agarwal N, Sonpavde G, Sartor O. Future Oncol. 2011; 7:15–24. [PubMed: 21174534]
4. Katz J, Janik JE, Younes A. Clin Cancer Res. 2011; 17:6428–6436. [PubMed: 22003070]
5. Krop I, Winer EP. Clin Cancer Res. 2014; 20:15–20. [PubMed: 24135146]
6. Ravelli RBG, Gigant B, Curmi PA, Jourdain I, Lachkar S, Sobel A, Knossow M. Nature. 2004; 428:198–202. [PubMed: 15014504]
7. Nogales E, Wolf SG, Downing KH. Nature. 1998; 391:199–203. [PubMed: 9428769]
8. David B, Sévenet T, Morgat M, Guénard D, Moisand A, Tollon Y, Thoison O, Wright M. Cell Motil Cytoskel. 1994; 28:317–326.
9. Batra JK, Powers LJ, Hess FD, Hamel E. Cancer Res. 1986; 46:1889–1893. [PubMed: 3948171]
10. Edler MC, Yang G, Jung MK, Bai R, Bornmann WG, Hamel E. Arch Biochem Biophys. 2009; 407:98–104. [PubMed: 19497297]
11. De Silva KT, Ratcliffe AH, Smith GF, Smith GN. Tetrahedron Lett. 1972; 10:913–916.

12. Thoison O, Guénard D, Sévenet T, Kan-Fan C, Quirion JC, Husson HP, Deverre JR, Chan KC, Potier P. C R Acad Sci Série II. 1987; 304:157–160.
13. Pascal C, Dubois J, Guénard D, Tchertanov L, Thoret S, Guéritte F. Tetrahedron. 1998; 54:14737–14756.
14. Buchanan R, Scozzie JA, Ariyan ZS, Heilman RD, Rippin DJ, Pyne WJ, Powers LJ. J Med Chem. 1980:1398–1405. [PubMed: 7452694]
15. Fogt SW, Scozzie JA, Heilman RD, Powers LJ. J Med Chem. 1980:1445–1448. [PubMed: 7452699]
16. Pyne, WJ.; Lowbridge, J.; Chang, IK.; Knotz, F.; Powers, LJ. European Patent Application. 81303611.8..
17. Mizens M, Brown WR, Laveglia J, Killeen JC Jr, Ignatoski J. Toxicologist. 1984; 4:17.
18. Mizens M, Brown WR, Killeen JC Jr, Ignatoski J. Toxicologist. 1985; 5:60.
19. de Aruda M, Cocchiaro CA, Nelson CM, Grinnell CM, Janssen B, Haupt A, Barlozzari T. Cancer Res. 1995; 55:3085–3092. [PubMed: 7606731]
20. Bai R, Edler MC, Bonate PL, Copeland TD, Pettit GR, Ludueña RF, Hamel E. Mol Pharmacol. 2009; 75:218–226. [PubMed: 18927208]
21. Gamble WR, Durso NA, Fuller RW, Westergaard CK, Johnson TR, Sackett DL, Hamel E, Cardellina JH II, Boyd MR. Bioorg Med Chem. 1999; 7:1611–1615. [PubMed: 10482453]
22. Hamel E, Lin CM. Biochemistry. 1984; 23:4173–4184. [PubMed: 6487596]
23. Grover S, Hamel E. Eur J Biochem. 1994; 222:163–172. [PubMed: 8200341]
24. Díaz JF, Barasoain I, Andreu JM. J Biol Chem. 2003; 278:8407–8419. [PubMed: 12496245]
25. Hamel E, Lin CM. J Biol Chem. 1984; 259:11060–11069. [PubMed: 6381495]
26. Bai R, Taylor GF, Schmidt JM, Williams MD, Kepler JA, Pettit GR, Hamel E. Mol Pharmacol. 1995; 47:965–976. [PubMed: 7746283]
27. Ponstingl H, Krauhs E, Little M, Kempf T. Proc Natl Acad Sci U S A. 1981; 78:2757–2761. [PubMed: 7019911]
28. Krauhs E, Little M, Kempf T, Hofer-Warbinek R, Ade H, Ponstingl H. Proc Natl Acad Sci U S A. 1981; 78:4156–4160. [PubMed: 6945576]
29. Lobert S, Vulevic B, Correia JJ. Biochemistry. 1996; 35:6806–6814. [PubMed: 8639632]
30. Rai SS, Wolff J. Eur J Biochem. 1997; 250:425–431. [PubMed: 9428694]
31. Ventilla M, Cantor CR, Shelanski ML. Arch Biochem Biophys. 1975; 171:154–162. [PubMed: 1238051]
32. Hodgkinson JL, Hutton T, Medrano FJ, Bordas J. J Struct Biol. 1992; 109:28–38. [PubMed: 1286008]
33. Jordan MA, Margolis RL, Himes RH, Wilson L. J Mol Biol. 1986; 187:61–73. [PubMed: 3959083]
34. Dabydeen DA, Florence GJ, Paterson I, Hamel E. Cancer Chemother Pharmacol. 2004; 53:397–403. [PubMed: 15060743]
35. Gapud EJ, Bai R, Ghosh AK, Hamel E. Mol Pharmacol. 2004; 66:113–121. [PubMed: 15213302]
36. Hamel E, Del Campo AA, Lowe MC, Lin CM. J Biol Chem. 1981; 256:11887–11894. [PubMed: 6117556]
37. Prota AE, Bargsten K, Northcote PT, Marsh M, Altmann KH, Miller JH, Díaz JF, Steinmetz MO. Angew Chem Int Ed. 2014; 53:1621–1625.
38. Hamel E, Day BW, Miller JH, Jung MK, Northcote PT, Ghosh AK, Curran DP, Cushman M, Nicolaou KC, Paterson I, Sorensen EJ. Mol Pharmcol. 2006; 70:1555–1564.
39. Pryor DE, O'Brate A, Bilcer G, Díaz JF, Wang Yu, Wang Yo, Kabaki M, Jung MK, Andreu JM, Ghosh AK, Giannakakou P, Hamel E. Biochemistry. 2002; 41:9109–9115. [PubMed: 12119025]
40. Gigant B, Wang C, Ravelli RBG, Roussi F, Steinmetz MO, Curmi PA, Sobel A, Knossow M. Nature. 2005; 435:519–522. [PubMed: 15917812]
41. Cormier A, Marchand M, Ravelli RB, Knossow M, Gigant B. EMBO Rep. 2008; 9:1101–1106. [PubMed: 18787557]
42. Wang Y, Benz FW, Wu Y, Wang Q, Chen Y, Chen X, Li H, Zhang Y, Zhang R, Yang J. Mol Pharmacol. 2016; 89:233–242. [PubMed: 26660762]

43. Timasheff SN, Andreu JM, Na GC. Pharmacol Ther. 1991; 52:191–210. [PubMed: 1818336]

Highlights

- (−)-Rhazinilam and NSC 613241 induce formation of spirals of different repeats.
- (−)-Rhazinilam and NSC 613241 do not bind avidly to microtubules or tubulin dimer.
- (−)-Rhazinilam and NSC 613241act substoichiometrically and synergistically.
- (−)-Rhazinilam and NSC 613241 do not inhibit each other's binding to spirals.
- Spiral formation : enhanced by GTP; inhibited by assembly inhibitors and by GDP.

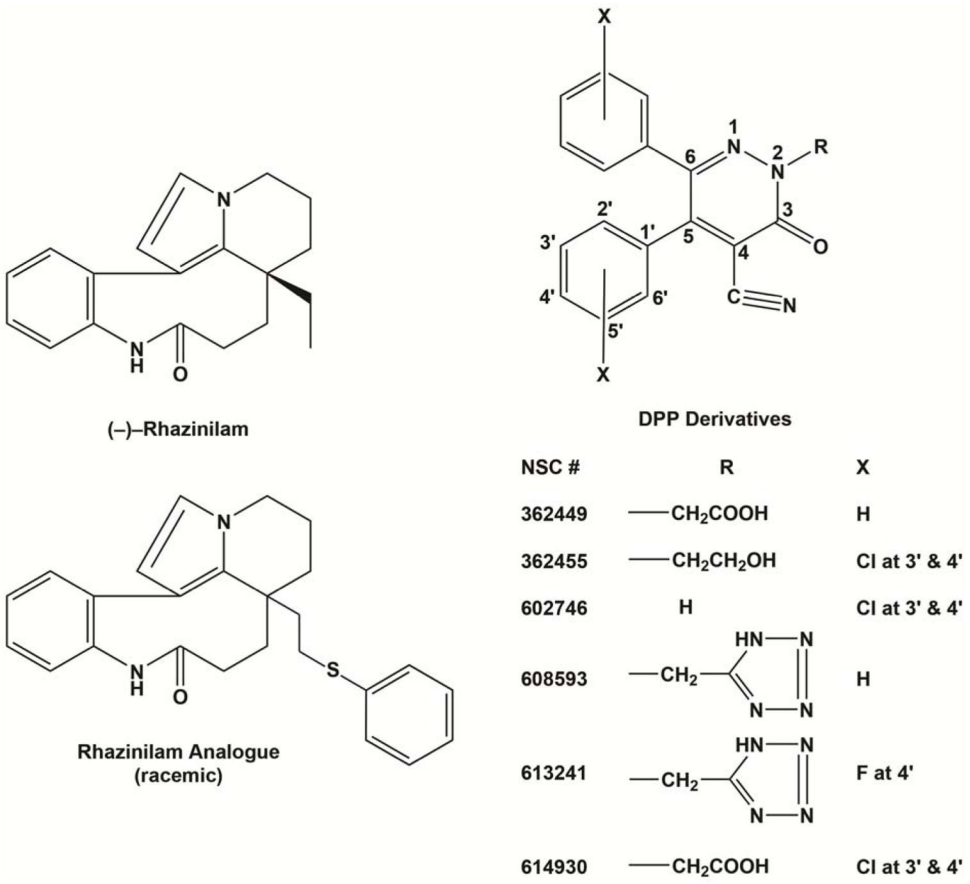

Fig. 1.

Structures of (−)-rhazinilam, a racemic rhazinilam analogue, and several DPP derivatives, including NSC 613241. IC_{50}'s for microtubule assembly for NSC 362449 and NSC 602746 were 6.2 ± 0.38 and 6.2 ±0.44 μM, respectively, obtained at the same time as the IC_{50} of 5.8 ± 0.23 μM was obtained for NSC 362455, as described in the text. These were the most active DPP derivatives described previously [9].

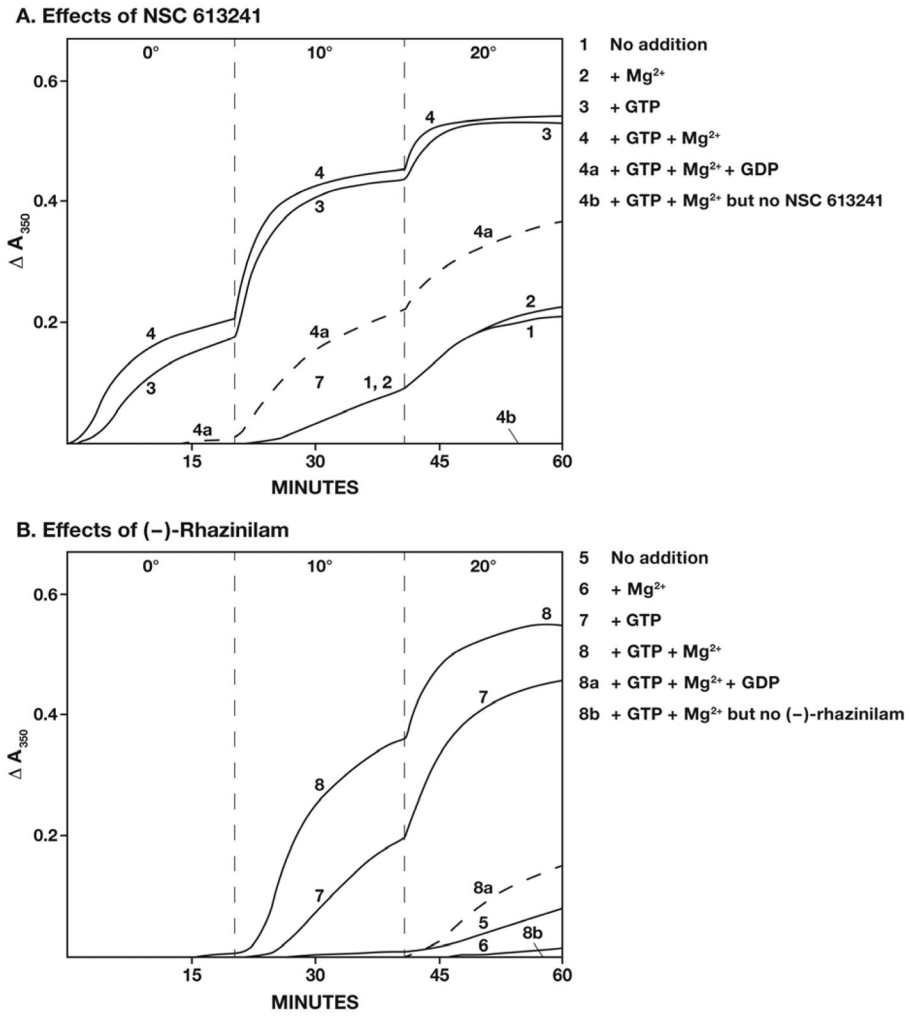

Fig. 2.

Aberrant tubulin assembly reactions induced by NSC 613241 (Panel A; curves 1–4) and (−)-rhazinilam (Panel B; curves 5–8). All reaction mixtures contained 10 μM tubulin, 0.6 M monosodium glutamate (pH 6.6), 2% dimethyl sulfoxide, and either 10 μM NSC 613241 or 10 μM (−)-rhazinilam, as indicated. There was no further addition to the reactions represented by curves 1 and 5. Further additions were 1.0 mM $MgCl_2$ only (curves 2 and 6), 50 μM GTP only (curves 3 and 7), both 1.0 mM $MgCl_2$ and 50 μM GTP (curves 4 and 8), and 1.0 mM $MgCl_2$, 50 μM GTP, and 500 μM GDP (dashed curves 4a and 8a). In addition, the arrows pointing to the baselines labeled curves 4b and 8b represent reaction mixtures containing 1.0 mM $MgCl_2$ and 50 μM GTP but no NSC 613241 (curve 4b) or no (−)-rhazinilam (curve 8b). Baselines at 350 nm were set with all components except NSC 613241 or (−)-rhazinilam mixed in the cuvettes. Addition of either NSC 613241 or (−)-rhazinilam, with rapid mixing into the reaction mixture, initiated the timing of the reaction. At the times indicated on the abscissa, the temperature was set at the temperatures indicated to the left of the dashed lines. Temperature rose in the cuvettes, once the temperature was set on the temperature controller at about 0.5 °C/s. It should be noted that 10 μM (−)-rhazinilam had no significant absorbance at 350 nm, whereas 10 μM NSC 613241 had absorbance of

about 0.1 A_{350} unit. This sudden jump when the cuvette chamber was closed could be readily distinguished from the increase in turbidity that began 30–60 s later.

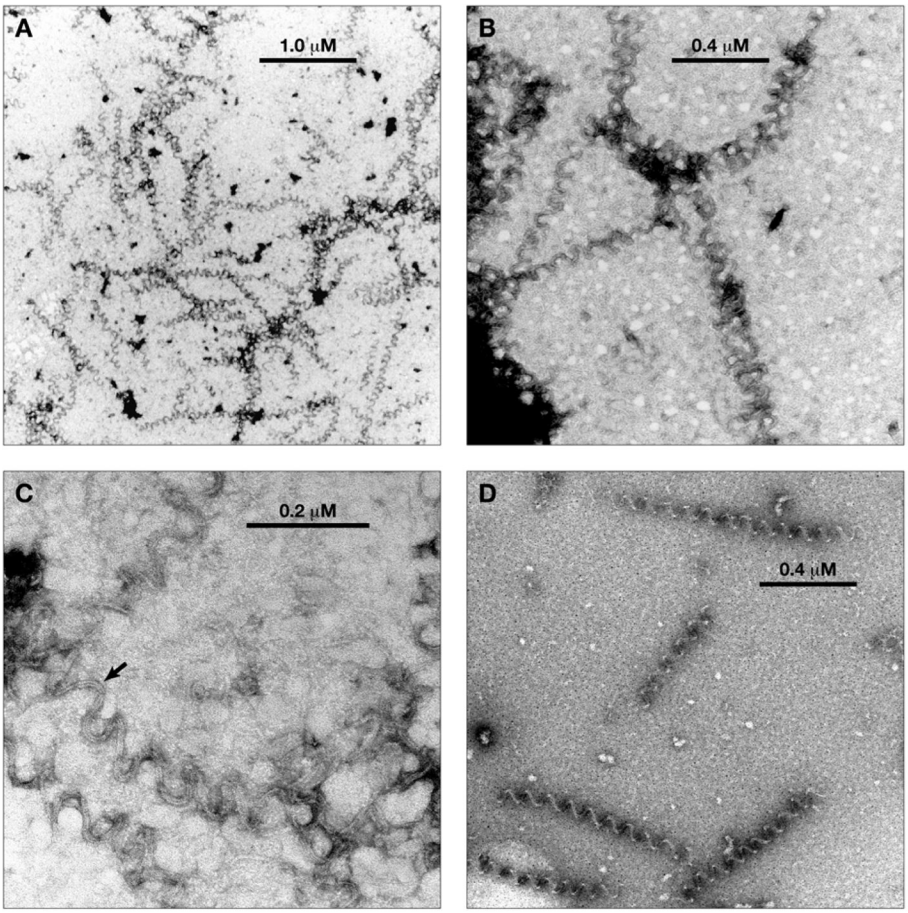

Fig. 3.

Electron micrographs of aberrant polymer formed with (−)-rhazinilam. Magnification is indicated by the bars in each panel. A. Lower magnification view. B. Middle magnification view. C. Higher magnification view. The arrow indicates a segment of polymer where a 2 filament substructure is clearly visible. D. Middle magnification view of polymer mildly fixed with glutaraldehyde (0.2%) before sample was applied to the grid.

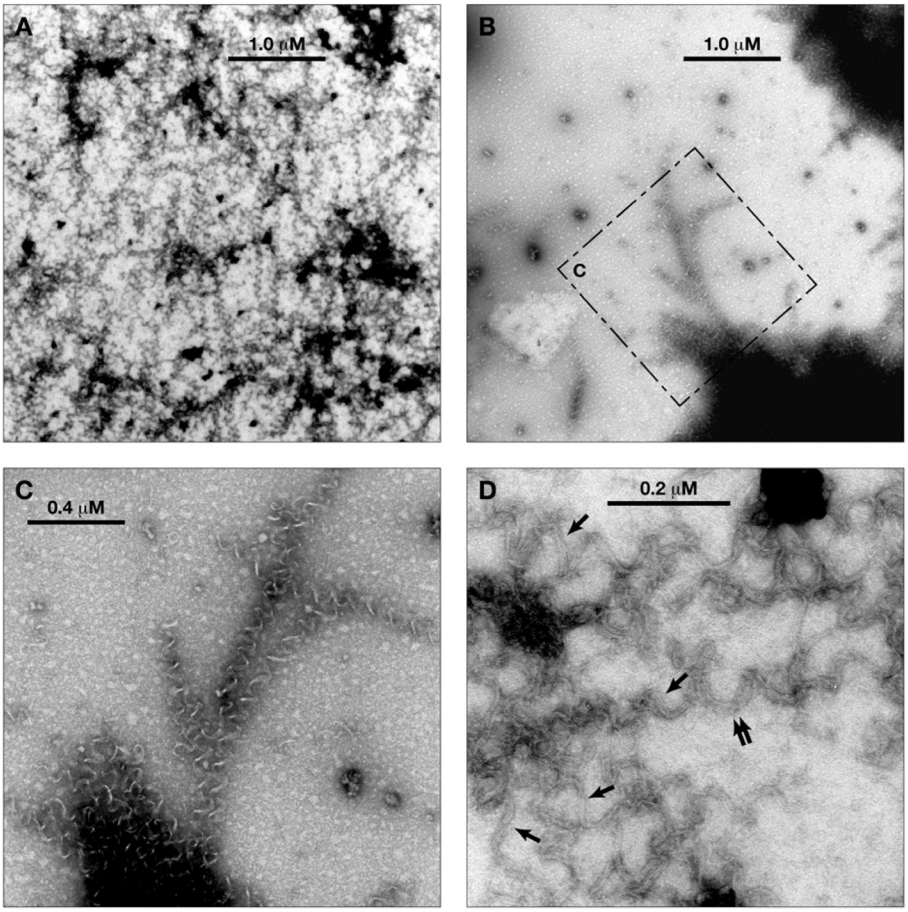

Fig. 4.

Electron micrographs of aberrant polymer formed with NSC 613241. Magnification is indicated by the bars in each panel. A and B. Lower magnification views. The dashed box in panel B indicates an area shown at higher magnification in panel C. C. Middle magnification view. D. Higher magnification view. Single arrows indicate areas with a 2 filament substructure. The double arrow indicates an area where there appears to be a 3 filament substructure, although this may be caused by overlapping spirals.

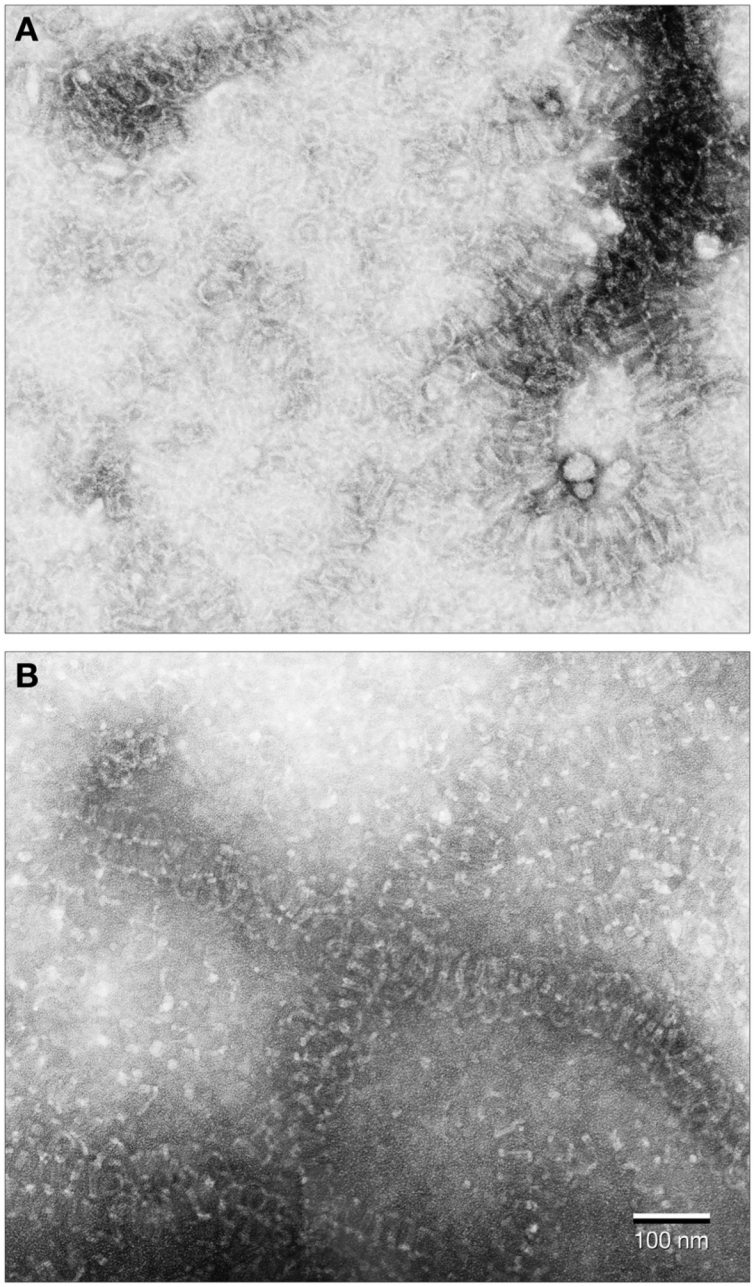

Fig. 5.

Electron micrographs of aberrant polymer formed with vinblastine in the absence (A) and presence of GTP (B). Reaction mixtures contained 10 μM tubulin, 0.75 M monosodium glutamate, 20 μM vinblastine, and, if present, 10 μM GTP. The tubulin used in these studies was not subjected to gel filtration chromatography.

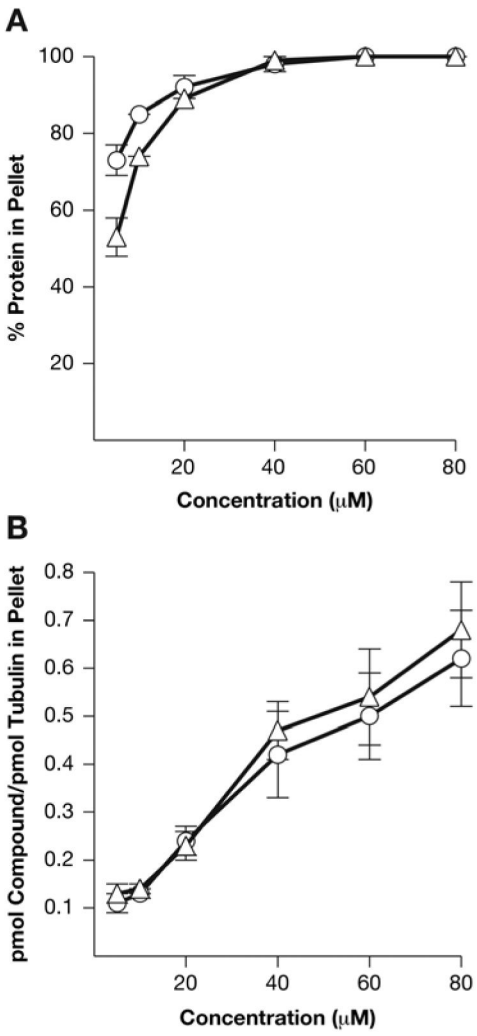

Fig. 6.

Concentration effects of (−)-rhazinilam and NSC 613241 on amount of tubulin in sedimentable polymer (A) and on stoichiometry of compounds in sedimentable polymer (B). Experimental details are described in detail in the text. In brief, reaction mixtures containing the indicated concentrations of [^{3}H](−)-rhazinilam (triangles) or [^{3}H]NSC 613241 (circles) were incubated at 22 °C for 30 min, and the polymer was harvested by centrifugation. Protein and radiolabel content of the pellets was determined, and these data were used to calculate the values shown in the Figure.

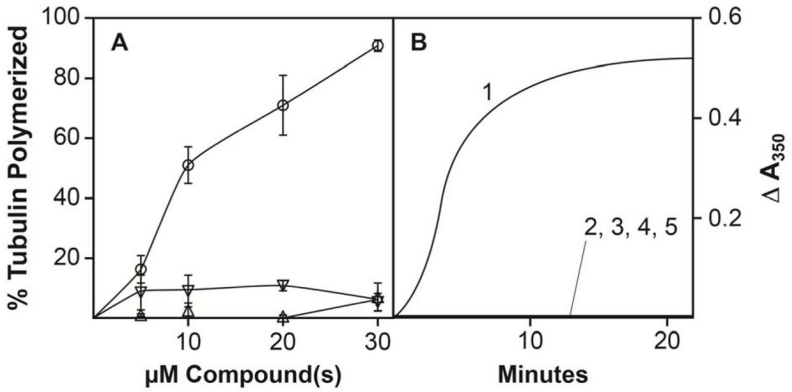

Fig. 7.

Both (−)-rhazinilam and NSC 613241 are required for aberrant assembly at 0 °C in the absence of GTP. Reaction mixtures contained 10 μM tubulin, 0.6 M monosodium glutamate (pH 6.6), 1.0 mM $MgCl_2$, 4% dimethyl sulfoxide, and NSC 613241 and/or (−)-rhazinilam, as indicated. A. Aberrant polymer harvested by ultracentrifugation as described in the text following a 20 min incubation at 0 °C. Symbols: circles, (−)-rhazinilam and NSC 613241 at the indicated concentrations; upright triangles, (−)-rhazinilam at the indicated concentrations; inverted triangles, NSC 613241 at the indicated concentrations. B. Formation of aberrant polymer by turbidimetry. Reactions were followed at 0 °C in a Gilford 250 spectrophotometer equipped with an electronic temperature controller. Curve 1, 15 μM (−)-rhazinilam and 15 μM NSC 613241; curve 2, 15 μM (−)-rhazinilam; curve 3, 30 μM (−)-rhazinilam; curve 4, 15 μM NSC 613241; curve 5, 30 μM NSC 613241.

Table 1

Inhibitors of microtubule assembly – effects on the aberrant polymerization reactions induced by (−)-rhazinilam and NSC 613241

Compound	Inhibits (−)-rhazinilam reaction		Inhibits NSC 613241 reaction			Independent aberrant	That confounds interpretation	
	At 10 °C	At 20 °C	At 0 °C	At 10 °C	At 20 °C	assembly reaction	Of (−)-rhazinilam rxn	Of NSC 613241 rxn
Podophyllotoxin	Yes[a]	Yes[a]	Yes[a]	Yes[a]	Yes[a]	No	NM[b]	NM[b]
Thiocolchicine[c]	Yes	Yes	Yes	Yes	No	Yes	No	No
Combretastatin A-4	Yes	No	Yes	Yes	No	No	NM[b]	NM[b]
Nocodazole	Yes	Yes	Yes[a]	Yes[a]	Yes[a]	Yes	No	No
Vinorelbine	Yes[a]	Yes[a]	Yes[a]	Yes[a]	Yes[a]	No	NM[b]	NM[b]
Vinblastine	No[d]	No[d]	Yes	Yes	No	Yes	Yes	No
Vincristine	No[d]	No[d]	Yes	Yes	No	Yes	Yes	No
Maytansine	Yes[a]	Yes[a]	Yes[a]	Yes[a]	Yes[a]	No	NM[b]	NM[b]
Dolastatin 10	Yes	Yes	Yes	Yes	Yes	Yes	No	No
Cryptophycin 1	Yes	Yes	Yes	No	No	No	NM[b]	NM[b]
Hemiasterlin	Yes[a]	Yes[a]	Yes[a]	Yes[a]	Yes[a]	No	NM[b]	NM[b]
Dolastatin 15	Yes	No	Yes	Yes	No	No	NM[b]	NM[b]
Pentapeptide[e]	Yes	Yes	Yes	Yes	Yes	Yes	No	No
Halichondrin B	Yes[a]	Yes[a]	Yes[a]	Yes[a]	Yes[a]	No	NM[b]	NM[b]
Spongistatin 1	Yes[a]	Yes[a]	Yes[a]	Yes[a]	Yes[a]	No	NM[b]	NM[b]

[a] Complete inhibition (no change in turbidity for 20 min at the indicated temperature).

[b] Not meaningful, since indicated agent caused no aberrant assembly reaction, as indicated by a change in apparent absorption at 350 nm, under the reaction conditions used in the experiment.

[c] Because of the relatively slow, temperature-dependent binding of thiocolchicine to tubulin, thiocolchicine was preincubated with tubulin to form the stable tubulin-thiocolchicine complex. Tubulin at 5.0 mg/mL with 500 μM thiocolchicine was incubated for 1 h at 37 °C in 1.0 M monosodium glutamate (pH 6.6), 1 mM $MgCl_2$, 5% dimethyl sulfoxide, and 0.4 mM GTP. The reaction mixture was chilled on ice and frozen in liquid nitrogen. For this experiment, control tubulin was incubated under the same reaction conditions without thiocolchicine (the control tubulin solution became turbid, due to assembly, but reclarified when placed on ice). Both solutions were examined at 1.0 mg/mL tubulin with addition of 10 μM (−)-rhazinilam or 10 μM NSC 613241.

[d] Aberrant assembly reactions induced by vinblastine and vincristine make it difficult or impossible to evaluate potential inhibition of the reactions induced by (−)-rhazinilam and NSC 613241. See the turbidity curves presented in the Supplemental Material.

[e] *N,N*-dimethylvalyl-valyl-*N*-methylvalyl-prolyl-proline.

Table 2

Binding of [^{3}H]paclitaxel or [^{3}H]peloruside A, but not [^{3}H](−)-rhazinilam or [^{3}H]NSC 613241 to gMTs[a]

Radiolabeled ligand[b]	Potential inhibitor[c]	Ligand bound/tubulin in gMTs ± SD
Paclitaxel		0.53 ± 0.094
Paclitaxel	Epothilone B	0.16 ± 0.043
Paclitaxel	Laulimalide	0.50 ± 0.018
Paclitaxel	(−)-Rhazinilam	0.62 ± 0.17
Paclitaxel	NSC 613241	0.59 ± 0.24
Peloruside A		0.67 ± 0.12
Peloruside A	Epothilone B	0.78 ± 0.033
Peloruside A	Laulimalide	0.088 ± 0.0023
Peloruside A	(−)-Rhazinilam	0.69 ± 0.039
Peloruside A	NSC 613241	0.63 ± 0.030
(−)-Rhazinilam		0.038 ± 0.0071
NSC 613241		0.035 ± 0.014

[a]Reaction mixtures (100 μL) contained 0.25 mg/mL gMTs (equivalent to 2.5 μM tubulin), 3.4 M glycerol, 6.0 mM $MgCl_2$, 1.0 mM GTP, 1.0 mM EGTA, 10 mM phosphate buffered saline (pH 6.8), 3% dimethyl sulfoxide, and radiolabeled ligand and inhibitor as indicated. Incubation was at room temperature (about 22 °C) for 10 min, and centrifugation was at 45,000 rpm for 10 min at 22 °C. Pellets were dissolved in 110 μL 8.0 M urea. Radiolabel and protein (Lowry assay) were each determined on 50 μL of the urea solution.

[b]Radiolabeled ligands, all tritiated, were at 2.5 μM. [c]Potential inhibitors, all nonradiolabeled, were at 25 μM.

Table 3

(−)-Rhazinilam and NSC 613241 do not appear to affect each other's binding to aberrant polymer[a]

Radiolabeled ligand	Potential inhibitor	Ligand bound/tubulin in aberrant polymer ± SD (% tubulin recovered in pellet)
10 μM (−)-Rhazinilam		0.37 ± 0.053 (37 ± 5.1)
10 μM (−)-Rhazinilam	80 μM NSC 613241	0.32 ± 0.022 (89 ± 6.4)
10 μM NSC 613241		0.15 ± 0.013 (72 ± 5.4)
10 μM NSC 613241	80 μM (−)-rhazinilam	0.16 ± 0.014 (95 ± 5.2)

[a]Experimental conditions were as described in the text. In brief, reaction mixtures containing the indicated concentrations of [^{3}H](−)-rhazinilam, [^{3}H]NSC 613241, nonradiolabeled NSC 613241, or nonradiolabeled (−)-rhazinilam were incubated at 22 °C for 30 min, and the polymer was harvested by centrifugation. Protein and radiolabel content of the pellets was determined, and these data were used to calculate the values shown in the Table.

Table 4

Both a DPP and (−)-rhazinilam or a rhazinilam analogue are required for polymer formation without GTP at 0 °C[a]

Compound(s) added	% tubulin in polymer ± SE
(−)-Rhazinilam[b]	0 ± 2
Racemic rhazinilam analogue[c]	0 ± 3
NSC 613241[b]	0 ± 2
NSC 608593[b]	0 ± 1
(−)-Rhazinilam[d]; racemic rhazinilam analogue[c]	0 ± 2
NSC 613241[d]; NSC 608593[d]	0 ± 2
(−)-Rhazinilam[d]; NSC 613241[d]	69 ± 3.0
(−)-Rhazinilam[d]; NSC 608593[d]	72 ± 1.4
Racemic rhazinilam analogue[b]; NSC 613241[d]	17 ± 1.9
Racemic rhazinilam analogue[b]; NSC 608593[d]	19 ± 3.8

[a]Reaction mixtures contained 1.0 mg/mL tubulin, 0.6 M monosodium glutamate (pH 6.6), 1.0 mM $MgCl_2$, compounds at the indicated concentrations, and 4% dimethyl sulfoxide. Incubation was for 20 min at 0 °C, with centrifugation as described in the text. The protein concentration in the supernatants was compared to the protein concentration in uncentrifuged samples to determine the % tubulin in the polymer pellets.

[b]Compound concentrations were 30 μM.

[c]Compound concentrations were 60 μM.

[d]Compound concentrations were 15 μM.